University of Massachusetts - Amherst
ScholarWorks@UMass Amherst

Astronomy Department Faculty Publication Series | Astronomy

2011

DETECTION OF STRONG MILLIMETER EMISSION FROM THE CIRCUMSTELLAR DUST DISK AROUND V1094 SCO: COLD AND MASSIVE DISK AROUND A T TAURI STAR IN A QUIESCENT ACCRETION PHASE?

T Tsukagoshi

M Saito

Y Kitamura

M Momose

Y Shimajiri

See next page for additional authors

Follow this and additional works at: http://scholarworks.umass.edu/astro_faculty_pubs

Part of the Astrophysics and Astronomy Commons

Tsukagoshi, T; Saito, M; Kitamura, Y; Momose, M; Shimajiri, Y; Hiramatsu, M; Ikeda, N; Kamegai, K; Wilson, G; Yun, Min; Scott, KS; Austermann, J; Perera, T; Hughes, D; Aretxaga, I; Mauskopf, P; Ezawa, H; Kohno, K; and Kawabe, R, "DETECTION OF STRONG MILLIMETER EMISSION FROM THE CIRCUMSTELLAR DUST DISK AROUND V1094 SCO: COLD AND MASSIVE DISK AROUND A T TAURI STAR IN A QUIESCENT ACCRETION PHASE?" (2011). *Astronomy Department Faculty Publication Series.* Paper 1143.
http://scholarworks.umass.edu/astro_faculty_pubs/1143

This Article is brought to you for free and open access by the Astronomy at ScholarWorks@UMass Amherst. It has been accepted for inclusion in Astronomy Department Faculty Publication Series by an authorized administrator of ScholarWorks@UMass Amherst. For more information, please contact scholarworks@library.umass.edu.

Authors
T Tsukagoshi, M Saito, Y Kitamura, M Momose, Y Shimajiri, M Hiramatsu, N Ikeda, K Kamegai, G Wilson, Min Yun, KS Scott, J Austermann, T Perera, D Hughes, I Aretxaga, P Mauskopf, H Ezawa, K Kohno, and R Kawabe

This article is available at ScholarWorks@UMass Amherst: http://scholarworks.umass.edu/astro_faculty_pubs/1143

arXiv:1011.0102v1 [astro-ph.SR] 30 Oct 2010

Detection of Strong Millimeter Emission from the Circumstellar Dust Disk Around V1094 Sco: Cold and Massive Disk around a T Tauri Star in a Quiescent Accretion Phase?

Takashi TSUKAGOSHI[1] Masao SAITO[2] Yoshimi KITAMURA[3] Munetake MOMOSE[4] Yoshito SHIMAJIRI[5,6] Masaaki HIRAMATSU[7,8] Norio IKEDA[3] Kazuhisa KAMEGAI[3] Grant WILSON[9] Min S. YUN[9] Kimberly SCOTT[9] Jay AUSTERMANN[9] Thushara PERERA[9] David HUGHES[10] Itziar ARETXAGA[10] Philip MAUSKOPF[11] Hajime EZAWA[5] Kotaro KOHNO[1,12] and Ryohei KAWABE[5]

ABSTRACT

We present the discovery of a cold massive dust disk around the T Tauri star V1094 Sco in the Lupus molecular cloud from the 1.1 millimeter continuum observations with AzTEC on ASTE. A compact ($r \lesssim$320 AU) continuum emission coincides with the stellar position having a flux density of 272 mJy which is largest

[1]Institute of Astronomy, Faculty of Science, University of Tokyo, Osawa 2-21-1, Mitaka, Tokyo, 181-0015, Japan: ttsuka@ioa.s.u-tokyo.ac.jp

[2]National Astronomical Observatory of Japan, Osawa 2-21-1, Mitaka, Tokyo 181-8588, Japan

[3]Institute of Space and Astronautical Science, Japan Aerospace Exploration Agency, Yoshinodai 3-1-1, Sagamihara, Kanagawa 229-8510, Japan

[4]Institute of Astrophysics and Planetary Sciences, Ibaraki University, Bunkyo 2-1-1, Mito 310-8512, Japan

[5]Nobeyama Radio Observatory, Nobeyama 462-2, Minamimaki, Minamisaku, Nagano 384-1305, Japan. Nobeyama Radio Observatory (NRO) is a branch of the National Astronomical Observatory of Japan (NAOJ)

[6]Department of Astronomy, School of Science, University of Tokyo, Hongo 7-3-1, Bunkyo, Tokyo 113-0033, Japan

[7]Academia Sinica Institute for Astronomy and Astrophysics, P.O. Box 23-141, Taipei 10617, Taiwan

[8]Institute of Astronomy, National Tsing Hua University, 101 Section 2 Kuang Fu Road, Hsinchu 30013, Taiwan

[9]Department of Astronomy, University of Massachusetts, Amherst, MA 01003

[10]Instituto Nacional de Astrofísica, Óptica y Electrónica, Luis Enrique Erro #1, Tonantzintla, Puebla, México

[11]Department of Physics and Astronomy, Cardiff University, Cardiff CF24 3YB, Wales, UK

[12]Research Center for the Early Universe, School of Science, University of Tokyo, 7-3-1 Hongo, Bunkyo, Tokyo 113-0033, Japan

among T Tauri stars in Lupus. We also present the detection of molecular gas associated with the star in the five-point observations in ^{12}CO J=3–2 and ^{13}CO J=3–2. Since our ^{12}CO and ^{13}CO observations did not show any signature of a large-scale outflow or a massive envelope, the compact dust emission is likely to come from a disk around the star. The observed SED of V1094 Sco shows no distinct turnover from near infrared to millimeter wavelengths, which can be well described by a flattened disk for the dust component, and no clear dip feature around 10 μm suggestive of absence of an inner hole in the disk. We fit a simple power-law disk model to the observed SED. The estimated disk mass ranges from 0.03 to $\gtrsim$0.12 $M_{\odot}$, which is one or two orders of magnitude larger than the median disk mass of T Tauri stars in Taurus. The resultant temperature is lower than that of a flared disk with the well-mixed dust in hydrostatic equilibrium, and is probably attributed to the flattened disk geometry for the dust which the central star can not illuminate efficiently. From these results together with the fact that there is no signature of an inner hole in the SED, we suggest that the dust grains in the disk around V1094 Sco sank into the midplane with grain growth by coalescence and is in the evolutional stage just prior to or at the formation of planetesimals.

Subject headings: stars: circumstellar matter — stars: individual(V1094 Sco — solar system: formation

1. Introduction

Protoplanetary disk around pre-main sequence stars are potential sites for planet formation. In the standard model (e.g. Hayashi et al. 1985), after settling into equilibrium, the gas and solid components in the disk are separated and dust grains begin sinking to the midplane to form a thin dust layer which eventually fragments into planetesimals, ingredients of planets. The radial profile of the surface density structure at this stage is likely one of the most important parameters to control what kinds of planets form in the disk (Kokubo & Ida 2002).

Since the gas and dust are well mixed in the beginning, the grain growth and sedimentation are key processes to separate dust from gas. Theoretical studies have suggested that dust grains are removed from the flaring surface and will sink to the midplane with growing by coalescence along the disk evolution (Dullemond & Dominik 2004; Tanaka et al. 2005). One way to find such evolved disks is to carefully examine the Spectral Energy Distribution (SED) of young stars as well as detection of (sub)millimeter continuum emission, because

the shape of the SED of young stars is sensitive to its temperature structure mainly determined by the vertical distribution of dust grains (Chiang & Goldreich 1997). Tanaka et al. (2005) studied the dust growth and settling in passive disks to investigate the evolution of disk structure and SEDs. Their numerical results indicated that the flux densities at mid-infrared (MIR) from a disk get lower as a result of dust grain growth and settling from the surface layer.

In the last two decades, extensive observations from optical to millimeter wavelengths have been conducted to study disk properties ultimately determining the nature of forming planets. Pre-main sequence stars, particularly in the quiescent phase such as weak line T Tauri stars (WTTSs) or Class III stars are good candidates for searching such evolved dusty disks in the process of sedimentation. A pioneer survey in (sub)millimeter continuum emission of the circumstellar dust around young stars was conducted by Beckwith et al. (1990) and followed by many other groups (Andre & Montmerle 1994; Osterloh & Beckwith 1995; Nuernberger et al. 1997; Kitamura et al. 2002; Andrews & Williams 2005, 2007). Kitamura et al. (2002) made an imaging survey of single T Tauri stars in Taurus and derived the physical properties of the disks combined with the SEDs. They found the radial expansion of the disks attributed to outward transport of angular momentum with decreasing Hα line luminosity, a measure of disk evolution. Andrews & Williams (2005) made a large survey of disk emission of more than 100 young stars in Taurus and found that there is a distinct difference in detection rates between classical T Tauri star (CTTS; 90%) and WTTS (15±5%). No massive evolved disk around WTTS, however, was found.

In the present paper, we report the discovery of an unusual cold massive disk around the T Tauri star, V1094 Sco, at the southern tip of Lupus 3 at a distance of 150 pc. The source has a quiescent accretion disk presumably in the transient stage from CTTS to WTTS because its equivalent width of Hα ranged 7–14 Å (Krautter et al. 1997; Wichmann et al. 1999). V1094 Sco is known as a single star whose spectral type, mass, and age are K6, 0.78 $M_{\odot}$, and 3 Myr, respectively (Wichmann et al. 1997).

2. Observations

Our observations have been performed with the Atacama Submillimeter Telescope Experiment (ASTE), the 10 m submillimeter telescope operated by Nobeyama Radio Observatory (NRO), a branch of National Astronomical Observatory Japan (NAOJ), in collaboration with University of Chile, and Japanese institutes including University of Tokyo, Nagoya University, Osaka Prefecture University, Ibaraki University, and Hokkaido University. The telescope is located at Pampa la Bola, Chile, an altitude of 4860m, and is remotely operated from

the ASTE operation facilities in Chile and Japan through the network observation system N-COSMOS3 (Kamazaki et al. 2005). We employed two receivers, AzTEC 1.1 mm camera (Wilson et al. 2008) and CATS345 receiver (Inoue et al. 2008), for millimeter continuum observations and molecular line observations at submillimeter wavelengths, respectively.

2.1. Millimeter Continuum Observations with AzTEC

AzTEC is a 144-element bolometer array camera installed on the ASTE between April 2007 and December 2008 (Wilson et al. 2008). In this period, the array was configured to operate at a wavelength of 1.1 mm. The angular resolution and field of view of AzTEC on ASTE were 28″and 7.′8, respectively.

We have made wide-field (40′×40′) millimeter continuum observations of the Lupus 3 molecular cloud including the target, V1094 Sco, in July 2007. The individual on-the-fly maps were obtained in the raster-scan mode with a scanning velocity of 100″ s^{-1}. The telescope was scanned along the AZ-EL coordinates with a spacing of 1.′95, a quarter of the field of view. All the data were taken at night or early morning and the average 270 GHz radiometric opacity at zenith was $\sim$ 0.05 during the observation period. Telescope pointing was checked by mapping the quasar J1517-243 every one and half, or two hours. The pointing corrections are applied during the data analysis. The flux conversion factor from optimal loading to source flux density of the AzTEC array was calibrated by observing Uranus, Neptune, or 3C279 every night.

The AzTEC data set was reduced by using the AzTEC Data Reduction Pipeline (Scott et al. 2008) for the identification of point sources. Following Scott et al. (2008), we employed the Principle Component Analysis (PCA) cleaning method to remove the atmospheric emission. The pixel size of the final map was set to be 3″, 10 % of AzTEC beam size. The noise level and effective resolution of the final map are 5.0 mJy $beam^{-1}$ and 35″, respectively.

2.2. Sub-Millimeter Molecular Line Observations with CATS345

^{12}CO and ^{13}CO J=3–2 line observations were performed in March 2008 with a 2 sideband-separating (2SB) receiver, CATS345, on ASTE. The half power beam widths (HPBWs) at 345.79 and 330.59 GHz were 22″ and 23″, respectively, which corresponds to 3300 and 3450 AU at the distance to the target. The main beam efficiency was about 60 % around these frequencies. The system noise temperatures were typically 400 and 350 K for ^{12}CO and ^{13}CO, respectively. For the backend, we used a 1024 channel digital auto-correlator, which

has a band width of 128 MHz and a resolution of 125 kHz, corresponding to 111 and 0.11 km s^{-1}, respectively, at 345 GHz. The telescope pointing calibration was performed every 1.5-2 hours by observing CRL 4211, and the resulting pointing accuracy was typically $3''$. For the absolute flux calibration, the integrated intensities of M17 SW and IRC 10216 were measured two or three times per day and compared with those by Wang et al. (1994). Data reduction and analysis were made with the NEWSTAR software package developed in NRO, which is a frontend of the Astronomical Image Processing System (AIPS) developed in the National Radio Astronomy Observatory (NRAO).

We employed the five-point observation method in which spectra are obtained not only at a stellar position but also at four adjacent points $22''$ apart from the stellar position in the R.A. or Dec. direction. This method enables us to deduce the excess emission toward the central star by subtracting the average spectrum of the surrounding four spectra from the central spectrum, even if the star is located in extended components, such as an ambient cloud.

3. Results of the Continuum Observations

The 1.1 mm continuum map around V1094 Sco is shown in Figure 1a. Strong compact continuum emission was detected towards the stellar position. From the 2-d Gaussian fitting, the peak position of the emission is obtained to be $16^{\rm h}08^{\rm m}36\overset{\rm s}{.}1$, $-39^\circ23'1\overset{''}{.}6$ in J2000, which agrees well with the 2MASS position of V1094 Sco within $1\overset{''}{.}5$. The total flux density at 1.1 mm was measured to be 272.1±7.6 mJy from the deconvolved cleaned map (see below), which is one of the strongest 1.1 mm emission among T Tauri stars in the Lupus molecular cloud. The negative contours around the emission are due to a point spread function (i.e., a beam; see Figure 1c) with a negative hole generated from the PCA cleaning method.

Figure 1b shows a deconvolved map by subtracting the measured point spread function (PSF) from the emission via the *clean* algorithm. The PSF of the AzTEC map for V1094 Sco is shown in Figure 1c. From the deconvolved map, we found that the emission is composed largely of a spatially unresolved component. The derived clean components are located around the star over two pixels ($3'' \times \sqrt{2} \sim 4\overset{''}{.}2$ in size) with its separation comparable to the pointing uncertainty estimated from the pointing measurements (Figure 1b). Therefore, we consider that the strong millimeter emission comes from a compact ($r \leq 4\overset{''}{.}2/2 = 320$ AU) circumstellar dusty disk associated with V1094 Sco. This is supported by the fact that, unlike the case of a stellar type flare seen in WTTS (Güdel 2002), V1094 Sco did not show any time variation of the flux density at millimeter wavelengths during the observing period.

Figure 2 shows the SED of V1094 Sco. The flux density at 1.1 mm is unusually strong as the 1.1 mm to infrared flux density ratio is near unity and larger than those for T Tauri stars in Taurus (Strom et al. 1989; Beckwith et al. 1990). Adapting the extinction relation of Rieke & Lebofsky (1985), we measured the spectral index for the dereddened fluxes in the range from 2 to 10 μm, $\alpha_{2,10}$, to be -1.39 ± 0.10, where $\alpha = [d\log(\lambda F_\lambda)/d\log(\lambda)]$. This value suggests that V1094 Sco should be categorized as a Class II object. The shape of the measured SED is unique in the sense that there are not distinct broadband spectral features, such as a large dip, from near-infrared (NIR) to millimeter wavelengths with a power-law like monotonic decrease. The index of the decrease is measured to be -0.98 ± 0.02 in the range from 2 to 1100 μm. However, there is a small turnover around 10 μm, i.e., the index at the longer wavelength, from 20 to 1100 μm, follows nearly the entire trend to be -0.93 ± 0.03 while that from 2 to 10 μm is -1.39 ± 0.10. Furthermore, there is no dip feature in the NIR to MIR wavelength range caused by clearing material in the inner parts of the disk, such as GM Aur (Hughes et al. 2009).

4. Results of the Molecular Line Observations

The five-point spectra of the ^{12}CO and ^{13}CO J=3–2 emissions are shown in Figure 3. The significant ^{12}CO and ^{13}CO emissions were detected over the five-points around the star. There is a clear intensity gradient along the east–west direction in the ^{13}CO spectra as well as in ^{12}CO. In the ^{12}CO spectra, we could not find any symmetrical wing feature of an outflow with a velocity width of $\sim$10 km s^{-1} which is often seen around a low-mass young stellar object. The ^{12}CO and ^{13}CO spectra are peaked around the LSR velocity of 4.9 km s^{-1}, which is slightly shifted from the systemic velocity of the Lupus III main cloud (4.1 km s^{-1}; Tachihara et al. 1996). The peak intensity in $T_{\rm MB}$ scale and the velocity width in FWHM are 7.0 K and 0.66 km s^{-1}, respectively, on average over the five-points for ^{12}CO, and 0.7 K and 0.85 km s^{-1} for ^{13}CO.

From the intensity ratio of the ^{12}CO to ^{13}CO spectra, we estimate the optical depth of both lines toward the star. If we assume the same excitation temperature, the mean optical depths of ^{12}CO and ^{13}CO are obtained to be 16.7 and 0.19, respectively. Since the ^{13}CO emission is optically thin in contrast to ^{12}CO, the associated gas with the star can be expected to be seen in ^{13}CO through the parent cloud as excess emission towards the star.

By assuming the local thermodynamic equilibrium with the excitation temperature, $T_{\rm ex}$, the H_2 mass of the gas in the beam solid angle toward the source, $M_{\rm H_2}$, can be estimated

from the intensity of the optically thin ^{13}CO J=3–2 line as follows:

$$\begin{aligned} M_{\rm H_2} &= 1.99\times10^{-14}\frac{1}{X_{^{13}\rm CO}}\left(\frac{D}{[\rm pc]}\right)^2 \\ &\times \frac{\exp(15.9/T_{\rm ex})}{1-\exp(-15.9/T_{\rm ex})}\frac{T_{\rm ex}}{J(T_{\rm ex})-0.05} \\ &\times \frac{\tau_{^{13}\rm CO}}{1-\exp(-\tau_{^{13}\rm CO})}\int\frac{T_{\rm A}^{*}(^{13}\rm CO)}{\eta_{\rm MB}}dv \qquad [M_\odot], \end{aligned} \tag{1}$$

where $J(T_{\rm ex}) = T_0/[\exp(T_0/T_{\rm ex})-1]$, $T_0 = h\nu/k_{\rm B}$, $X_{^{13}\rm CO}$ is the fractional abundance of ^{13}CO with respect to H_2, D is the distance to the source, τ is the optical depth, and $\eta_{\rm MB}$ is the main beam efficiency of ASTE (Scoville et al. 1986). We adopt an excitation temperature 10 K which is the typical value in the ambient molecular cloud (Vilas-Boas et al. 2000), and 1.7×10^{-6} for $X_{^{13}\rm CO}$ by assuming that the abundance ratio of ^{12}CO/^{13}CO and the H_2/^{12}CO conversion factor are 60 and 10^4, respectively. Our mass as well as column density are estimated to be 6.7×10^{-3} $M_\odot$ and 1.2×10^{21} cm^{-2} by using equation (1). The column density is much smaller than the averaged one in the Lupus 3 cloud (Tachihara et al. 1996), suggesting that there is no large and massive envelope around V1094 Sco.

To search for the compact excess emission towards the star, we made residual spectra of the ^{12}CO and ^{13}CO emission as shown in Figure 4. Each residual spectrum was obtained by subtracting the average of the surrounding four spectra from the central one. The excess emission above the 2σ noise level over two velocity channels can be discerned in the ^{13}CO residual spectrum around the velocity of 6 km s^{-1}. The peak intensity and the velocity width in FWHM are measured to be 0.12 K and 1.43 km s^{-1}, respectively. Since the velocity of the excess emission agrees well with the radial velocity of the star, 5.8±1.0 km s^{-1} (Guenther et al. 2007), this may be the possible detection of the gas disk around V1094 Sco.

The ^{12}CO residual emission was detected at $V_{\rm LSR}$ = 4.1 and 6.4 km s^{-1} whose peak intensities are 0.30 and 0.43 K in $T_{\rm MB}$, respectively. Although the ^{12}CO emission is shown to be optically thick, the double-peaked profile of the residual spectrum towards the star might suggest the presence of a rotating gas disk around V1094 Sco. We tried to fit the rotating disk model (Kitamura et al. 1993) to the both spectra to examine quantitatively. We could not, however, find any parameter set to reproduce the both residual spectra consistently. For example the ^{12}CO intensity can be reproduced for the larger rotating disk model. Such a disk model expects the stronger ^{13}CO intensity than the obtained and can not explain the both intensities compatibly. In addition, both velocity widths are not well fitted by the model simultaneously. Consequently, the residual spectrum in ^{12}CO is not likely to originate from the circumstellar gas disk.

5. Discussion

5.1. Analysis of Spectral Energy Distribution

The measured SED of V1094 Sco has the unique feature: there is no significant turnover and a monotonic decrease from NIR to millimeter. This feature is well described by a flattened disk for the dust component. According to Chiang & Goldreich (1997), the flattened disk has a lower temperature than that of a flared disk with the well-mixed dust because the central star can not illuminate the flattened disk efficiently. In this case, the SED is predicted to have an asymptotic power-law slope with an index of $n = 4/3$ from 30 μm to 1 mm. The MIR to millimeter continuum radiation mainly comes from the optically thick interior of the disk. On the other hand, the SED of a flared disk rises in the MIR to far-infrared (FIR) regime owing to the strong emission from a hot surface layer and gradually falls down toward the millimeter regime, mainly tracing the cooler interior.

To deduce disk parameters, we performed the least square fitting to the SED of V1094 Sco using a simple power-law disk model (same as model 1 case in Kitamura et al. 2002). Our disk model is assumed to have a power-law form of the surface density and temperature variations over the entire area of the disk, $\Sigma(r)$ and $T(r)$, respectively:

$$\Sigma(r) = \Sigma_{100\mathrm{AU}} \left(\frac{r}{[100\mathrm{AU}]} \right)^{-p} \tag{2}$$

and

$$T(r) = T_{1\mathrm{AU}} \left(\frac{r}{[1\mathrm{AU}]} \right)^{-q}. \tag{3}$$

Here, r is the radial distance in units of AU, $\Sigma_{100\mathrm{AU}}$ is the surface density at 100 AU, and $T_{1\mathrm{AU}}$ is the temperature at 1 AU. We applied the model to the data without the extinction correction because it was corrected in the model by calculating the mass opacity at each frequency from A_{v} with the extinction curve (figure 1 of Adams et al. 1988). The lower limit of the temperature is fixed at 10 K which is the typical temperature of the Lupus 3 cloud (Vilas-Boas et al. 2000). We adopt the effective temperature of the star of 4255 K, the stellar mass of 0.78 $M_{\odot}$ and the visual extinction toward the star of 1.75 mag (Wichmann et al. 1997). The outer radius of the disk, R_{out}, and the disk inclination angle, i, are fixed to be 320 AU and 45 degree, respectively. The outer radius is derived from the pixel size of $3''$ as an upper limit because the emission was not spatially resolved. Stellar radius, R_*, inner radius of the disk, R_{in}, $T_{1\mathrm{AU}}$, q and $\Sigma_{100\mathrm{AU}}$ are the free parameters of the disk model. The model SEDs are computed and fitted to the observational data for the following four cases: $p = 1$ and 1.5 (minimum mass solar nebula by Hayashi et al. 1985) and $\beta = 0$ and 1, where β is the power-law index of the dust mass opacity coefficient, $\kappa_\nu = 0.1 \times (\frac{\nu}{10^{12}\mathrm{Hz}})^{\beta}$ cm^2 g^{-1}

(Beckwith et al. 1990). In the fitting, we treated all the data points with the equal weights of the largest uncertainty because the SED fitting tends to be biased toward the data points with small uncertainties at shorter wavelengths.

These model SEDs seem to agree with the observed SED as shown in Figure 2 and its reduced chi-squares are measured to be ~ 9. The derived parameters by the fitting are listed in Table 1 and 2. In Figure 2, we plotted the fitting results only for $p = 1.5$ case because the two best-fit curves with $p = 1$ and 1.5 are almost identical for each β value. Two remarkable disk features are derived in the fitting. First, the disk is very cold with a temperature of 99 K at 1 AU. The fitted stellar luminosity of 0.85 $L_\odot$ suggests that $T_{1\mathrm{AU}}$ in the condition of radiative equilibrium is expected to be 269 K when the disk is in hydrostatic equilibrium and gas and dust are well mixed. Previous studies of the SED fitting have found that most T Tauri stars in Taurus have a higher temperature of 100–400 K at 1 AU (Kitamura et al. 2002; Andrews & Williams 2005). Our derived low temperature suggests a flattened dust disk as predicted by theoretical studies (e.g. Chiang & Goldreich 1997). The second remarkable finding is that the disk is massive. Our estimated disk mass ranges from 0.03 to 0.12 $M_\odot$ and the ratio of the disk to stellar mass is 3–13%. These values are much higher than the typical values for T Tauri stars in the Taurus-Auriga region: median disk masses are 4×10^{-3} and 2×10^{-3} $M_\odot$ for CTTS and WTTS, respectively, and the median disk-to-star mass ratio is only 0.5 % (Andrews & Williams 2005). It is very rare to find a massive disk in a quiescent accretion phase like a WTTS one. For example, Andrews & Williams (2005) have found that only 15 % of WTTSs are detectable at the submillimeter wavelengths.

The above arguments are not affected much by either the disk inclination angle or the disk outer radius. If we change the disk inclination angle from 20 to 70 degrees with $R_{\mathrm{out}} = 320$ AU and $p = 1.5$, the temperature at 1 AU varies from 90 to 128 K, which is still low, and the index q remains around 0.68. The variation of the disk mass is less than 20 %, remaining the massive disk. Furthermore, when we adopt a smaller R_{out} than 320 AU, a higher surface density is required to reproduce the observed SED, resulting the massive disk. For example, in the R_{out}=110 AU case, $\Sigma_{100\mathrm{AU}}$ becomes more than 5 times larger than that for the R_{out}=320 AU case and the disk mass increases up to 0.42 $M_\odot$, which remains massive. For a smaller opaque disk, we cannot accurately estimate the disk mass, though our interpretation of the massive disk is still valid. Therefore, we definitely conclude that the disk around V1094 Sco is colder than the usual flared disk and that the disk mass is much larger than the typical value of T Tauri stars in Taurus.

In our SED fitting, we adopted a low threshold of 10 K in the temperature profile because the source is likely embedded in its parent cloud as shown by our ^{12}CO observations. This threshold causes an increment of flux densities around at 300 μm in the model SED because

the temperature of 10 K corresponds to 290 μm by Wien's law (see Figure 2). To investigate the effect of the temperature threshold, we also analyzed the SED by using a disk model with a threshold of 2.7 K, the temperature for the cosmic background radiation. In this case, the observed SED can be well fitted only when the disk inclination angle is less than 30 degree. The fitted SED for $p = 1.5$ and $\beta = 0.0$ case is shown by a gray line in Figure 2; the best-fit curve can also explain the observed SED, and the disk mass becomes four times larger than that in the 10 K threshold case. Note that such a massive disk relative to the stellar mass is likely to be gravitationally unstable. On the other hand, $T_{1\mathrm{AU}}$ and q decrease only by 2 % and 11 %, respectively. Consequently, the threshold in the temperature profile of the disk model does not change our interpretation of a cold massive disk around V1094 Sco.

5.2. Rare Object to Provide the Initial Conditions of Planet Formation

The cold and massive disk we found around V1094 Sco strongly suggests the presence of a flattened disk where a large number of small dust grains are settling. Since V1094 Sco seems to be in the quiescent phase of disk accretion, the majority of dust particles are expected to just settle into the midplane with dust growth through coalescence. Theoretically, the thin dust layer in the midplane fragments into numerous planetesimals by its gravitational instability, and as a result, a hole appears at the inner part of the disk to produce a dip feature at ~ 10 μm in SED. However, we could not find such a feature at the IR wavelengths in the SED of V1094 Sco, indicating that there is no inner hole created by the formation of planetesimals. Indeed, the strong continuum emission toward V1094 Sco that we detected suggests that a large number of small particles rather than larger planetesimals with sizes of ~ 10 km is the dominant component in the circumstellar disk. Consequently, the disk around V1094 Sco is most likely in the quiescent stage after the dust sedimentation in the midplane, but just prior to the planetesimal formation.

V1094 Sco is a rare object in terms of the shape of its SED. To find a similar object with a massive cold disk to V1094 Sco, we checked the available photometric data at the MIR and millimeter wavelengths (Strom et al. 1989; Beckwith et al. 1990) and measured the flux ratio of MIR flux to millimeter flux. We found that only CY Tau, a Class II CTTS in Taurus, has a high intensity ratio of the 1 mm to 70 μm as well as to 25 μm (> 0.5), suggesting the strong millimeter flux despite its weak MIR flux and the SED with a monotonic slope from MIR to millimeter. The temperature at 1 AU and the disk mass of CY Tau are estimated to be 87 K and 0.13 $M_\odot$, respectively (Kitamura et al. 2002). We can roughly estimate the timescale for the duration of a cold and massive disk like those around V1094 Sco and CY Tau as follows. Given about 30 samples in Taurus whose flux densities at 1 mm and MIR were previously

determined, the timescale of the cold massive disk is estimated to be at least one order of magnitude shorter than the typical age of a T Tauri star ($\sim 1 \times 10^{6-7}$ yr), if we assume that new stars randomly form with a constant rate. Such a short timescale is consistent with the gravitational instability of the thin dust layer after the dust sedimentation at the midplane. It is suggested that the dust layer produced by settling to the equatorial plane becomes gravitationally unstable and rapidly fragments into numerous planetesimal ($\ll 10^5$ yrs; Dominik et al. 2007).

It is very interesting that the physical properties of such a quiescent disk provide the initial conditions of the successive formation of planets (e.g. Kokubo & Ida 2002). In particular, it is crucial to reveal the radial variation of the disk surface density with high-resolution and high-sensitive observations in future. For the dust coagulation, it is theoretically expected that the index of the dust opacity coefficient, β, is lower than unity as a result of dust growth (Miyake & Nakagawa 1993). We treated β as fixed parameter in the SED fitting because the photometric data at the millimeter and sub-millimeter wavelengths are limited. More (sub-)millimeter data are required to determine the β value accurately. Additionally, high-resolution molecular line observations will reveal the disk kinematics and the initial conditions of the planet forming disk more quantitatively.

6. Summary

We have detected the strong 1.1 mm continuum emission toward the T Tauri star, V1094 Sco, in the Lupus molecular cloud with AzTEC on ASTE. In addition, we have obtained the ^{12}CO and ^{13}CO J=3–2 spectra at the five positions around the source. The main results of our observations are summarized in the following.

- Significant continuum emission was detected just toward the stellar position. The emission is not spatially resolved with the effective ASTE beam size of 35″, indicating that a dust disk is associated with the star. The total flux density is 272 mJy at 1.1 mm which is the strongest among T Tauri stars in the Lupus molecular cloud.

- The ^{12}CO and ^{13}CO emissions were detected over the five-points around the star. The five-points spectra show no signature of a large-scale molecular outflow or a massive envelope. We made residual spectra by subtracting the average spectrum of the surrounding four spectra from the central spectra. The ^{12}CO excess emission was found and the ^{13}CO one was marginally discerned towards the star. The ^{13}CO excess may come from the gas disk while the ^{12}CO excess emission detected can not be explained by the gas disk.

- The observed SED shows two prominent features. First, there is no significant turnover with a constant slope from NIR to millimeter which is well reproduced by a flattened disk. Second, there is no signature of a dip at around 10 μm suggesting no inner hole in the disk.

- We fit a power-law disk model to the SED when p is fixed to be 1.0 and 1.5, and β is 0.0 and 1.0. The best fit parameters of the disk are $\Sigma_{100\mathrm{AU}}$ =(1.25–4.97) g cm^{-2}, $T_{1\mathrm{AU}}$ =99 K, q = 0.68, and M_{disk} =(0.03–0.12) $M_{\odot}$. The disk temperature at 1 AU is lower than that of a flared disk in hydrostatic equilibrium. The disk mass is much higher than the typical values for T Tauri stars.

- The cold and massive disk around V1094 Sco can be well interpreted as a partially settled disk of a large number of small dust grains. Together with no signature of an inner hole in the SED, it is most likely that the disk is in the quiescent phase after the dust sedimentation in the midplane, but just prior to the planetesimal formation. The V1094 Sco may be a rare sample to investigate the initial conditions for the formation of a planetary system.

We appreciate the referee for the constructive comments that have helped to improve this manuscript. We acknowledge the ASTE and AzTEC staff for the operation and maintenance of the observing instruments. We are grateful to S. Komugi, T. Minamidani, and K. Fukue for testing the data reduction software. We thank N. Ukita, B. Hatsukade, and S. Ikarashi for the pointing model correction of AzTEC on ASTE. Observations with ASTE were in part carried out remotely from Japan by using NTT's GEMnet2 and its partner R&E (Research and Education) networks, which are based on AccessNova collaboration of University of Chile, NTT Laboratories, and NAOJ. This work is supported in part by a Grant-in-Aid for Scientific Research (A) from the Ministry of Education, Culture, Sports, Science and Technology of Japan (No. 19204020) and by JSPS (No. 18204017).

REFERENCES

Adams, F. C., Shu, F. H., & Lada, C. J. 1988, ApJ, 326, 865

Andre, P., & Montmerle, T. 1994, ApJ, 420, 837

Andrews, S. M., & Williams, J. P. 2005, ApJ, 631, 1134

Andrews, S. M., & Williams, J. P. 2007, ApJ, 671, 1800

Beckwith, S. V. W., Sargent, A. I., Chini, R. S., & Guesten, R. 1990, AJ, 99, 924

Chiang, E. I., & Goldreich, P. 1997, ApJ, 490, 368

Cieza, L., et al. 2007, ApJ, 667, 308

Cutri, R. M., et al. 2003, The IRSA 2MASS All-Sky Point Source Catalog, NASA/IPAC Infrared Science Archive. http://irsa.ipac.caltech.edu/applications/Gator/,

The Denis Consortium 2005, VizieR Online Data Catalog, 1, 2002

Dominik, C., Blum, J., Cuzzi, J. N., & Wurm, G. 2007, Protostars and Planets V, 783

Dullemond, C. P., & Dominik, C. 2004, A&A, 421, 1075

Güdel, M. 2002, ARA&A, 40, 217

Guenther, E. W., Esposito, M., Mundt, R., Covino, E., Alcalá, J. M., Cusano, F., & Stecklum, B. 2007, A&A, 467, 1147

Hayashi, C., Nakazawa, K., & Nakagawa, Y. 1985, Protostars and Planets II, 1100

Hughes, A. M., et al. 2009, ApJ, 698, 131

Inoue, H., Muraoka, K., Sakai, T., Endo, A., Kohno, K., Asayama, S., Noguchi, T., & Ogawa, H. 2008, Ninteenth International Symposium on Space Terahertz Technology, 281

Kamazaki, T., et al. 2005, Astronomical Data Analysis Software and Systems XIV, 347, 533

Kitamura, Y., Omodaka, T., Kawabe, R., Yamashita, T., & Handa, T. 1993, PASJ, 45, L27

Kitamura, Y., Momose, M., Yokogawa, S., Kawabe, R., Tamura, M., & Ida, S. 2002, ApJ, 581, 357

Kokubo, E., & Ida, S. 2002, ApJ, 581, 666

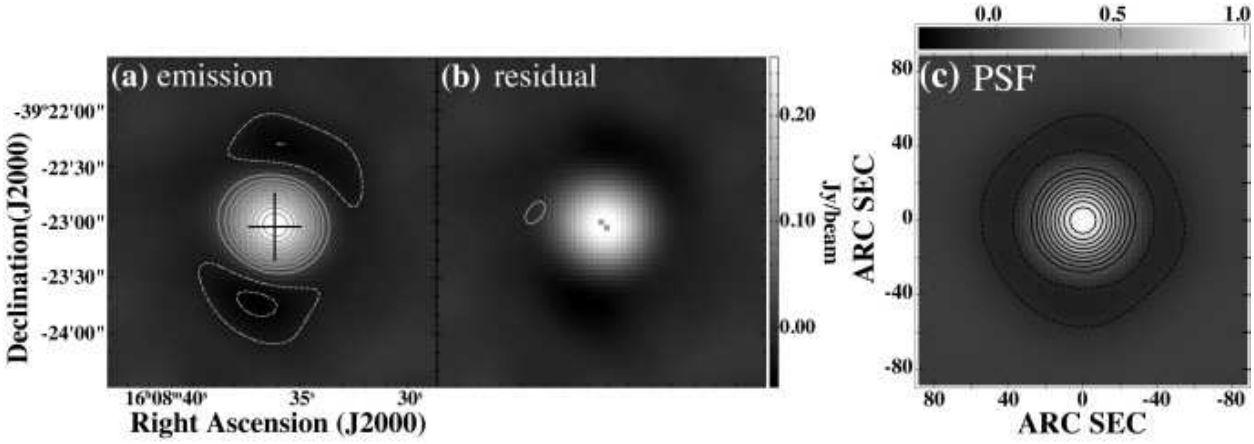

Fig. 1.— (a)1.1 mm continuum map of V1094 Sco obtained with AzTEC on ASTE. The contour lines start at $\pm 5\sigma$ with intervals of 5σ where 1σ is 5 mJy beam^{-1}. The negative levels are indicated by the dashed lines. The position of V1094 Sco is shown by the central cross. (b) The residual contour map by deconvolving the PSF via the clean algorithm is superposed on the continuum map (a) in grey scale. The contour levels and the grey scale are the same as in Figure 1(a). The shaded area indicates the positions of the clean components. (c) Point Spread Function (PSF) of the map (a) obtained with AzTEC on ASTE. The contour levels are $\pm 10\times$n % of the peak value (n=1,2,3,...). The negative levels are indicated by the dashed lines.

Table 1. Adopted parameters for SED fitting

parameter	value
$T_{\rm eff}$ [K]	4255
M_* [$M_\odot$]	0.78
$A_{\rm V}$ [mag]	1.75
$R_{\rm out}$ [AU]	320
i [degree]	45
p	1.0 & 1.5
β	0.0 & 1.0

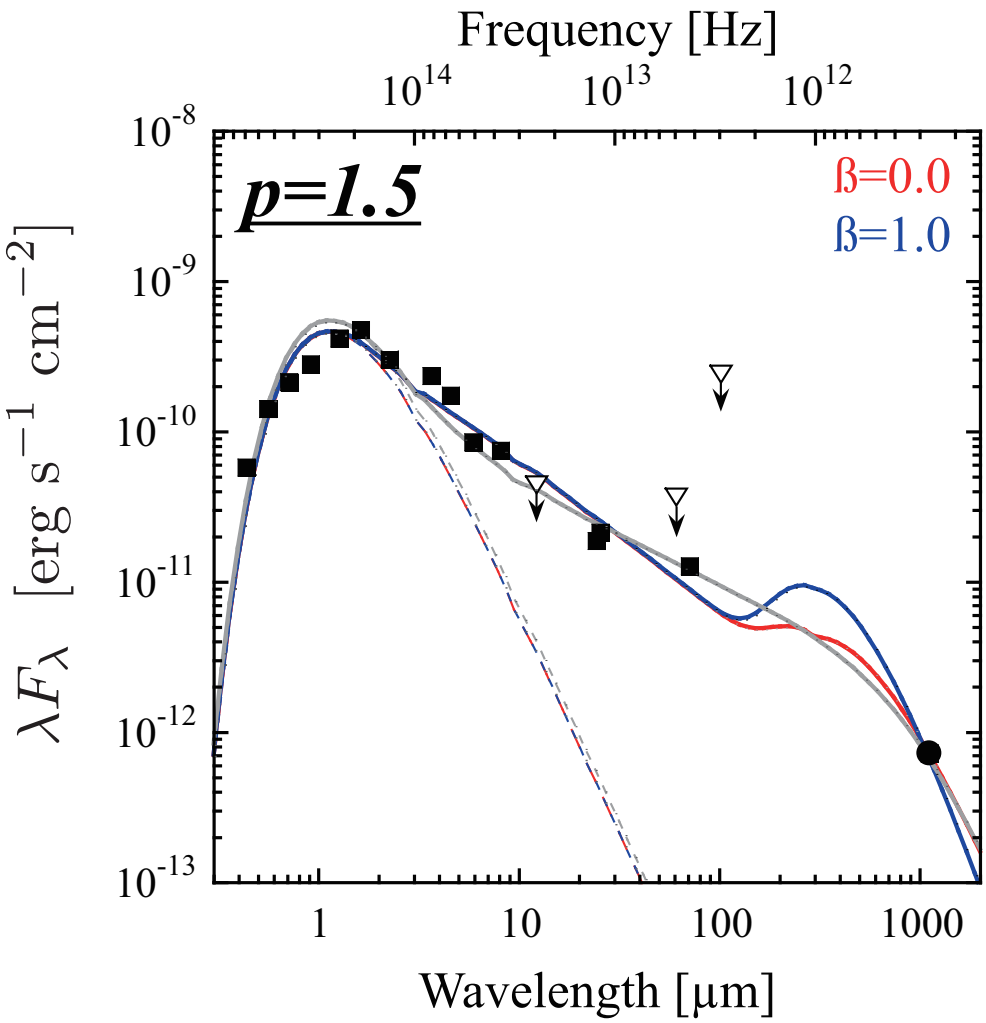

Fig. 2.— Spectral Energy Distribution (SED) of V1094 Sco. The result of our observations is shown in the filled circle. The filled squares indicate the SED compiled from previous studies; the NOMAD catalog (Zacharias et al. 2005), the DENIS database (The Denis Consortium 2005), the 2MASS point source catalog (Cutri et al. 2003), the *IRAS* faint source catalog (Moshir et al. 1992), and the spitzer photometry (3.6, 4.5, 5.8, 8.0, and 24 μm Cieza et al. 2007). The flux density at 70 μm with *Spitzer* MIPS was measured by analyzing the archived data using the program MOPEX/APEX software packages. The *IRAS* flux densities at 12, 60, and 100 μm are upper limits and shown by the open triangles. The dashed lines show the stellar contributions and the solid line show the best-fitted curves in the case of $p = 1.5$. The red and blue lines show the calculations for β =0 and 1, respectively. A grey line indicates the fitting results for the model disk with a low threshold temperature of 2.7 K in the temperature profile when $p = 1.5$ and $\beta = 0$.

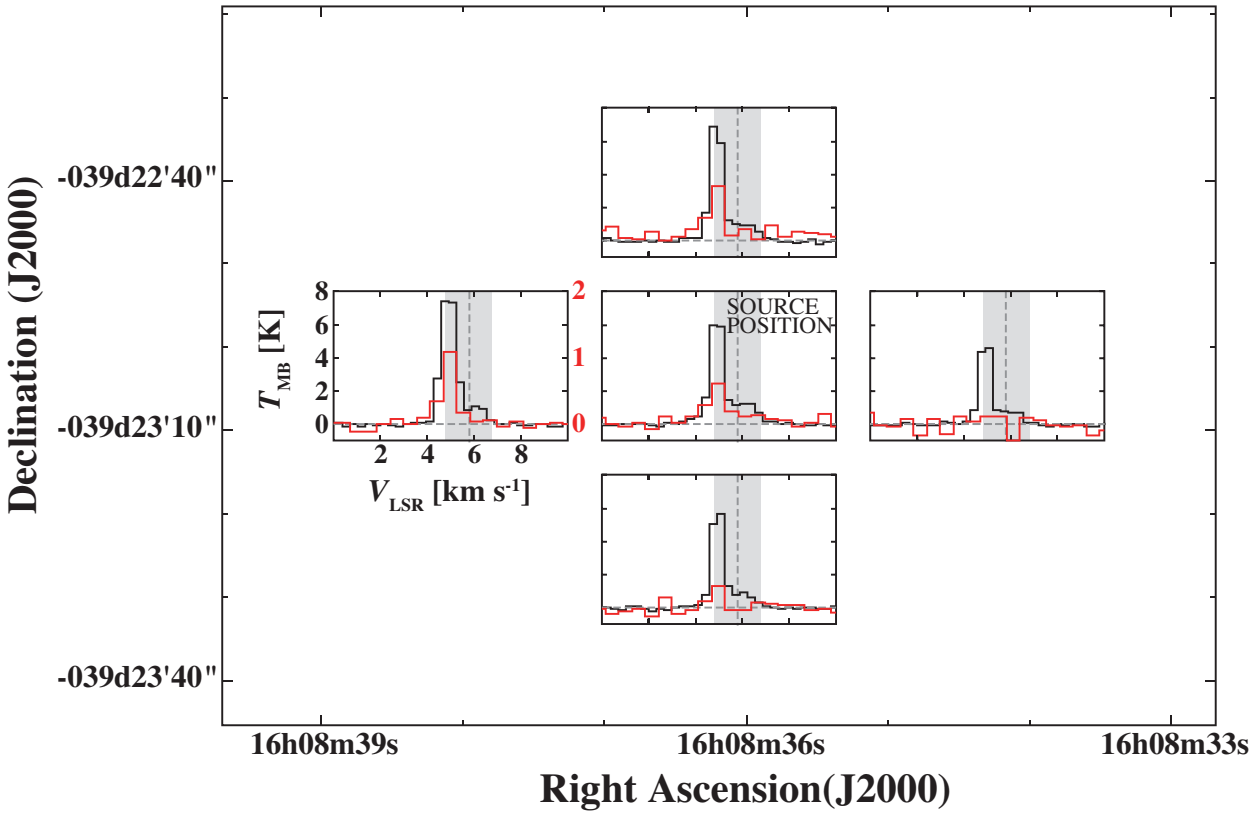

Fig. 3.— ^{12}CO (black) and ^{13}CO (red) J=3–2 five-point profile maps of V1094 Sco. The observed points are located at the stellar position, to the 22″ north, south, east, and west from the center. The spectra are smoothed in resolutions of 0.3 and 0.5 km s^{-1} for ^{12}CO and ^{13}CO, respectively. The shaded areas show the radial velocity of the central star with their error (Guenther et al. 2007).

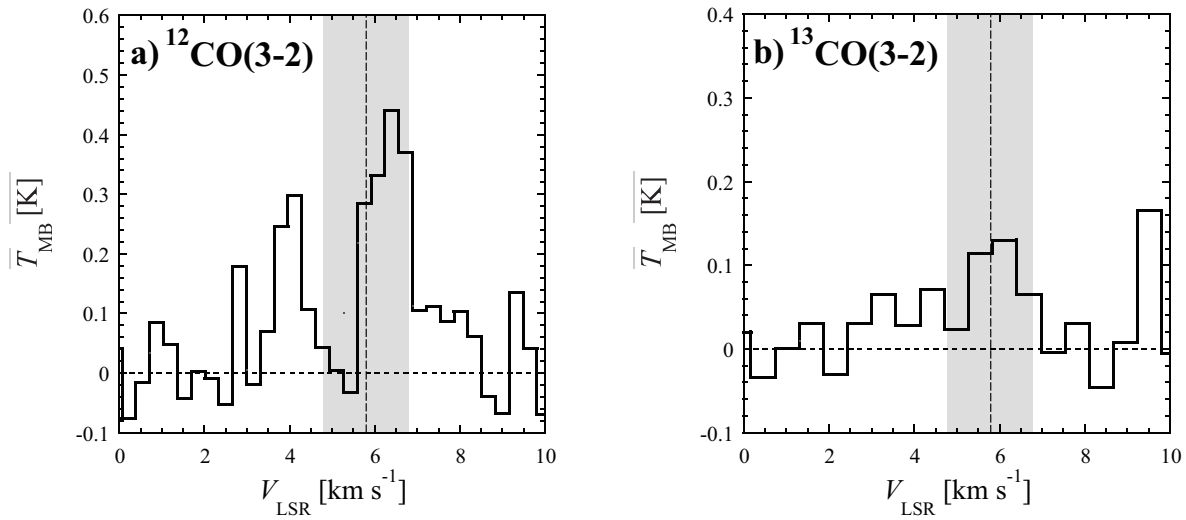

Fig. 4.— Residual spectra of ^{12}CO and ^{13}CO towards V1094 Sco. The vertical dotted lines and the shaded areas show the radial velocity of the star and its uncertainty (Guenther et al. 2007).

Table 2. Results of SED fitting

parameter	value			
β	0.0		1.0	
p	1.0	1.5	1.0	1.5
R_* [AU]	0.008			
L_* [$L_\odot$]	0.85			
$R_{\rm in}$ [AU]	0.02			
$\Sigma_{\rm 100AU}$ [g cm^{-2}]	1.25	1.47	4.31	4.97
$T_{\rm 1AU}$ [K]	99.0	99.0	99.3	99.4
q	0.68			
$M_{\rm disk}$ [$M_\odot$]	0.03	0.04	0.10	0.12

Krautter, J., Wichmann, R., Schmitt, J. H. M. M., Alcala, J. M., Neuhauser, R., & Terranegra, L. 1997, A&AS, 123, 329

Miyake, K., & Nakagawa, Y. 1993, Icarus, 106, 20

Moshir, M., Kopman, G., & Conrow, T. A. O. 1992, Pasadena: Infrared Processing and Analysis Center, California Institute of Technology, 1992, edited by Moshir, M.; Kopman, G.; Conrow, T. a.o.,

Nuernberger, D., Chini, R., & Zinnecker, H. 1997, A&A, 324, 1036

Osterloh, M., & Beckwith, S. V. W. 1995, ApJ, 439, 288

Papaloizou, J. C. B., Nelson, R. P., Kley, W., Masset, F. S., & Artymowicz, P. 2007, Protostars and Planets V, 655

Rieke, G. H., & Lebofsky, M. J. 1985, ApJ, 288, 618

Scott, K. S., et al. 2008, MNRAS, 385, 2225

Scoville, N. Z., Sargent, A. I., Sanders, D. B., Claussen, M. J., Masson, C. R., Lo, K. Y., & Phillips, T. G. 1986, ApJ, 303, 416

Strom, K. M., Strom, S. E., Edwards, S., Cabrit, S., & Skrutskie, M. F. 1989, AJ, 97, 1451

Tachihara, K., Dobashi, K., Mizuno, A., Ogawa, H., & Fukui, Y. 1996, PASJ, 48, 489

Tanaka, H., Himeno, Y., & Ida, S. 2005, ApJ, 625, 414

Vilas-Boas, J. W. S., Myers, P. C., & Fuller, G. A. 2000, ApJ, 532, 1038

Wang, Y., Jaffe, D. T., Graf, U. U., & Evans, N. J., II 1994, ApJS, 95, 503

Wichmann, R., Krautter, J., Covino, E., Alcala, J. M., Neuhaeuser, R., & Schmitt, J. H. M. M. 1997, A&A, 320, 185

Wichmann, R., Covino, E., Alcalá, J. M., Krautter, J., Allain, S., & Hauschildt, P. H. 1999, MNRAS, 307, 909

Wilson, G. W., et al. 2008, MNRAS, 386, 807

Zacharias, N., Monet, D. G., Levine, S. E., Urban, S. E., Gaume, R., & Wycoff, G. L. 2005, VizieR Online Data Catalog, 1297, 0

This preprint was prepared with the AAS LaTeX macros v5.2.